Biophysical Chemistry 6 (1977) 271–278

THERMOOSMOSIS THROUGH CHARGED MEMBRANES

Masayasu TASAKA, Shusaku ABE *
Department of Industrial Chemistry, Faculty of Engineering, Shinshu University, Wakasato, Nagano 380, Japan

and

Shinji SUGIURA ** and Mitsuru NAGASAWA
Department of Synthetic Chemistry, Faculty of Engineering, Nagoya University, Chikusa-ku, Nagoya 464, Japan

Received 30 November 1976

Thermoosmosis through oxidized collodion and collodion-sulfonated polystyrene interpolymer membranes has been observed in KCl solutions of various concentrations. The effective temperature difference acting for thermoosmosis was determined by measuring the thermal membrane potential appearing on both sides of membrane. It was found that the velocity of thermoosmosis is proportional to the effective temperature difference and the proportionality constant (thermo-osmotic coefficient) is a function of electrolyte concentration. The dependence of the thermoosmotic coefficient of charged-membranes on the electrolyte concentration is found to have a characteristic feature.

1. Introduction

Various membrane phenomena have extensively been studied in relation to biological phenomena. Study of non-isothermal membrane phenomena is also important to account for some biological phenomena such as the sensation of "warm and cold" [1]. Despite the fact that the effect of a temperature gradient on a membrane potential is now fairly well understood [2,3], it appears that no definite conclusions have been obtained about the effect of a temperature difference on the permeation of water and ions through membranes.

Various papers have been published on thermo-osmosis of electrolyte solutions through membranes but the conclusions obtained are not considered consistent. It was first reported by Carr and Sollner [4] that thermoosmosis through oxidized collodion membranes in KCl solutions occurs from the hot side to the cold side. Later, however, many papers have appeared in which the directions of thermoosmosis through phenolsulfonic acid membrane in 10^{-3} N HCl solution [5], through polystyrene membrane in toluene [5], through cellophane in methanol [6] and through sulfonated polyethylene cationic and anionic membranes in water [7] were all from the cold side to the hot side. Recently, Goldstein and Verhoff also reported that osmosis and solute flux in the thermo-osmosis experiments occurred from the colder solution to the warmer solution through polystyrene sulfonic acid cation exchange membrane in NaCl and $(CH_3)_4NCl$ solutions [8]. Moreover, the direction of thermoosmosis through potassium phenolsulfonate membrane in 10^{-3} M KCl solution [5] and through cellophane mambrane in water [6,9] varied with temperature, i.e., the direction was from the hot side to the cold side at lower temperatures and from the cold side to the hot side at higher temperatures.

One of the most important problems for obtaining quantitative data of thermoosmosis may be the measurement of the effective temperature difference acting for thermoosmosis. The effective temperature difference on both sides of a membrane may be entirely

* Present address: Niigata-Meikun High School, Kawagishi-cho, Niigata 951, Japan.
** Present address: Kansai Paint Co., Hiratsuka-Shi, Kanagawa 254, Japan.

Table 1
The properties of membranes

Membrane	Thickness δ (mm)	Water content, g of water/g of dry membrane	Concentration of fixed charges in the membrane (eq/cm^3)	Total drying time (min)	Drying temperature (°C)	Oxidation time (min)
o-m-1 [a]	1.12	–	–	120	5	13
o-m-2 [a]	0.53	3.3	–	190 [b]	25	10
o-m-3	0.63	–	–	95	25	15
c-m [a]	0.53	1.8	–	190 [b]	25	–
i-m-1	1.00	} 2.0 [12]	} 1×10^{-5} [12]	360 [b]	25	–
i-m-2	0.30			180 [b]	25	–

[a] Membranes o-m-1, o-m-2 and c-m are the same as in ref. [10].
[b] These membranes were dried in a loosely closed box.

different from the temperature difference in bulk solutions. In this work, the effective temperature difference on both sides of a membrane was determined by measuring the thermal membrane potential. Preliminary experimental data were previously reported at a symposium [10].

2. Experimental

2.1. Membranes

The oxidized collodion membranes used in this work were prepared according to the method of Sollner and his co-workers [11]. A collodion of Katayama Chemical Co., 1st grade, was poured on a glass plate and was dried for 95 to 190 minutes at room or low (ca. 5°C) temperature, depending upon the properties desired. These membranes were reinforced with wide-mesh cotton gauze. The membranes thus dried were immersed in distilled water to separate them from the glass plates. The membranes were oxidized in 1 M sodium hydroxide for 10–15 minutes and were washed with distilled water repeatedly. The properties of these membranes are listed in table 1. Membranes o-m-1, o-m-2 and o-m-3, prepared by controlling the drying and oxydation times, have similar transport numbers but have different thickness. The thin membranes o-m-2 and o-m-3 are used for observing thermoosmosis, while the thick membrane o-m-1 is used to determine the relationship between thermal membrane potential and temperature difference. Moreover, membrane c-m is an untreated collodion membrane and, therefore, it has little fixed charges. Membrane o-m-2 was prepared by oxidizing c-m. Comparison between the data with o-m-2 and c-m clarifies the effect of fixed charges. Unfortunately, however, the concentration of fixed charges in these oxidized collodions cannot be determined analytically.

Measurements with collodion-sulfonated polystyrene interpolymer membranes i-m-1 and i-m-2 were carried out for further theoretical analysis, since the concentration of fixed charges in these membranes can be experimentally determined. The properties of membranes i-m-1 and i-m-2 are also listed in table 1. These membranes were prepared to have properties similar to membrane C-1 in ref. [12].

The transport numbers of anion t_- in these membranes are shown as functions of the average KCl concentration, $[c(1) + c(2)]/2$, in fig. 1. They were calculated from the membrane potentials $\Delta\psi$ using the following approximate equation [2]:

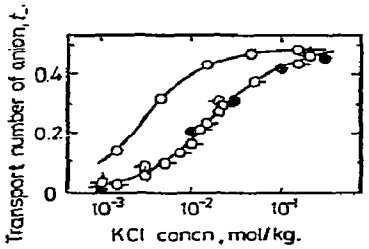

Fig. 1. The dependence of transport number of anion on KCl concentration for membranes o-m-1 (o-), o-m-2 (ó), o-m-3 (-o), c-m (o) and i-m-1 and i-m-2 (•).

$$\Delta\psi = (RT/F)(2t_- - 1) \ln [a_\pm(2)/a_\pm(1)]. \quad (1)$$

2.2. Measurement of the thermal membrane potential

The cell used for establishing the relationship between membrane potential and temperature difference on both sides of a membrane was almost the same as in refs. [2,3]. Two solutions at different temperatures are flushed on both surfaces of a thick membrane. The relationship between thermal membrane potential and temperature difference can be expressed by

$$-\Delta\psi = [(2t_+ - 1)(R/F) \ln a_\pm + (t_+\alpha_+ + t_-\alpha_-)]\,\Delta T, \quad (2)$$

where

$$\alpha_+ = \eta - s_+^0/F + \tau_0 s_0, \quad (3)$$

$$\alpha_- = \eta + s_-^0/F + \tau_0 s_0, \quad (4)$$

$$s_0 = s_0^0 - R \ln a_0 \quad (5)$$

and a_0 is the activity of water, s_i^0 the partial molar entropy, τ_0 the reduced transport number of water, and η is the differential thermoelectric potential coefficient.

It has been shown [2,3] that eq. (2) is in quantitative agreement with experimental results. By using the method reported previously [2,3], the constant α_+ for the present membranes can be determined from the data at low ionic strength with high reliability, but α_- must be chosen to fit the experimental data to eq. (2). The values of $\alpha_\pm$ thus estimated for the present membranes are $\alpha_+ = 0.26$ and $\alpha_- \approx -0.46$ mV/K. The values of $\Delta\psi/\Delta T$ calculated from eq. (2) using the data in fig. 1 together with these values of $\alpha_\pm$ are shown by solid lines in fig. 3. The satisfactory agreement between the calculated and observed values may confirm the reliability of the values of $\alpha_\pm$.

2.3. Determination of the effective temperature difference

If the electrolyte solutions cannot be flushed, the effective temperature difference on both sides of membrane may be considerably different from the temperature difference in bulk solutions, so that the thermal membrane potential may be much lower than the value predicted from eq. (2). In such cases, on the contrary, the effective temperature difference may be estimated from the thermal membrane potential observed [2,3]. That is, the constants in eq. (2) are first determined for a membrane by the method in section 2.2. The membrane potential appearing on both sides of the membrane through which thermoosmosis is observed is measured by connecting two calomel electrodes to the cell. Then, the effective temperature difference can be calculated from the membrane potential using eq. (2). The thick membrane is used for determining the constants in eq. (2), while the thin membrane is used in the thermoosmosis cell. It is theoretically predicted that the relationship between thermal membrane potential and effective temperature difference is independent of membrane thickness [2].

Moreover, there is another problem: The thermal membrane potential in the thermoosmosis cell cannot be measured, while thermoosmosis is being observed. In this work, therefore, the relationship between the effective temperature difference, ΔT, calculated from the thermal membrane potential, and the temperature difference in two bulk solutions, ΔT_b, is first established for each membrane at the same experimental conditions as when thermoosmosis is measured. The reproducibility in $\Delta T/\Delta T_b$ is considerably good. The effective temperature difference during thermoosmosis can thus be estimated from the temperature difference in two bulk solutions, using the ratio of $\Delta T/\Delta T_b$. The electrostatic potential differences in both the thermal membrane potential cell and the thermoosmosis cell were measured by a potentiometer of type K2 and a galvanometer.

2.4. Measurements of thermal hydrostatic pressure difference, thermoosmosis and hydraulic permeation

The cell was constructed of two chambers made of poly(methylmethacrylate) resin and the upper hot chamber was larger than the lower cold chamber as shown in fig. 2. The system is unstable if the temperature in the lower chamber is higher than that in the upper chamber. The hot chamber has an on–off thermoregulator with electrical heater to maintain a constant temperature (±0.01 K). The temperature in the cold chamber was kept at about 298 ± 0.05 K by a glass tube cooler, through which a constant-temperature cold water (±0.01 K) was circulated. A magnetic stirrer was used in the cold chamber. The volume flow was calculated from the movement of the meniscus in a

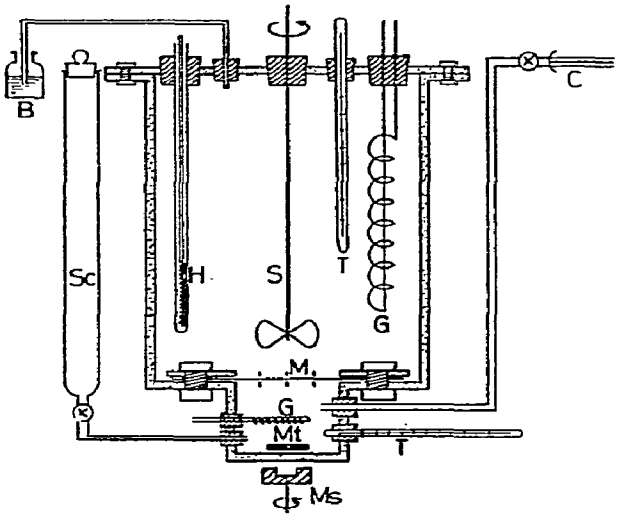

Fig. 2. The apparatus for measurement of thermoosmosis. B, bottle to adjust the solution level; C, capillary tube; G, glass tube for circulating cold water; H, heater; M, membrane; Ms, magnetic stirrer; Mt, magnetic stirrer tip; S, stirrer; Sc, solution container; T, thermometer.

capillary connected with the lower chamber. The diameter of the capillary was about 1mm. To prevent bending of the membrane, three thin plates of poly-(methylmethacrylate) resin of about 3 mm in height were in parallel cemented with the resin frames, as shown in fig. 2. Moreover, rubber gaskets of 1 mm in thickness with an internal opening of 5 cm in diameter was placed between the poly(methylmethacrylate) resin blocks.

The thermal hydrostatic pressure difference was measured using a vertical capillary. Several hours were required to reach the equilibrium height. The zero solution level in the capillary was determined from the direction of water flow by changing the relative heights in both chambers. As the movement of the solution was not very sensitive to the change in solution levels, the zero level was determined as the mid-point in the range where no solution flow could be observed.

The hydraulic permeation velocity of electrolyte solutions was also determined in the same apparatus by applying a pressure difference on both sides of the membrane.

To determine the thermal membrane potential in the thermoosmosis cell, two saturated KCl bridges are inserted into the holes for capillaries in the upper and the lower half-cells and connected with calomel electrodes.

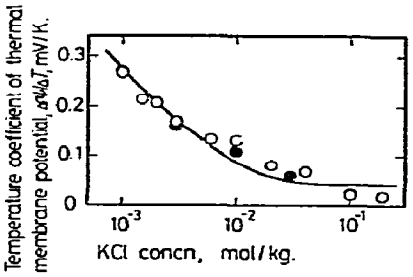

Fig. 3. The dependence of temperature coefficient of thermal membrane potential through membranes o-m-1 (○) and i-m-1 (●) on KCl concentration. The solid line denotes the values of $\Delta\psi/\Delta T$ calculated from eq. (2), assuming $\alpha_+ = 0.26$ and $\alpha_- = -0.46$ mV/K.

3. Results and discussion

3.1. Thermal membrane potential and effective temperature difference

When two electrolyte solutions at different temperatures are flushed on both surfaces of membranes o-m-1 and i-m-1, the membrane potential $\Delta\psi$ was found to vary linearly with the temperature difference ΔT, as reported in refs. [2,3]. The slopes obtained, $\Delta\psi/\Delta T$, are plotted against logarithmic activity of KCl in fig. 3. The curve of $\Delta\psi/\Delta T$ versus $\log a_\pm$ deviates from the theoretical linear line with slope 2.303 R/F because of the decrease of the transport number with increasing concentration of KCl [2]. It seems coincidental that both data for o-m-1 and i-m-1 fit the same curve. Since membranes o-m-2, o-m-3 and i-m-2 have the same transport numbers t_+ as o-m-1 and i-m-1, respectively, it can be assumed that the relationships between $\Delta\psi/\Delta T$ and $\log a_\pm$ in fig. 3 hold for membranes o-m-2, o-m-3 and i-m-2, too.

The thermal membrane potential in the thermoosmosis apparatus, where the electrolyte solutions cannot be flushed, was determined with membranes o-m-2, o-m-3 and i-m-2. By calculating the effective temperature differences ΔT from the thermal membrane

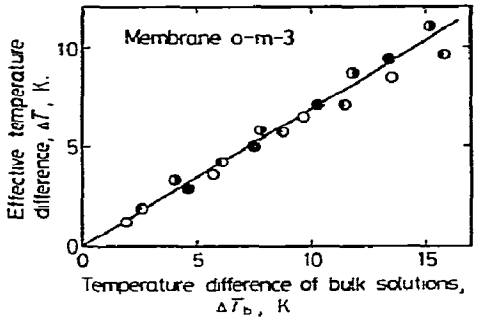

Fig. 4. The relationship between ΔT and ΔT_b with membrane o-m-3. KCl concentrations (mol/kg): ○, 0.001; ◑, 0.003; ◐, 0.02; ●, 0.2.

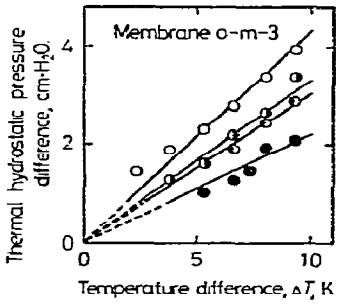

Fig. 5. The thermal hydrostatic pressure difference through membrane o-m-3. KCl concentrations (mol/kg): ●, 0.003; ◐, 0.02; ◑, 0.2; ○, 0.75.

potentials using the relationship in fig. 3, we can determine $\Delta T/\Delta T_b$ for each membrane at various KCl concentrations. If the stirring conditions were not changed, the ratio $\Delta T/\Delta T_b$ was found to be independent of electrolyte concentration within experimental error. An example of the relationship between ΔT and ΔT_b is shown in fig. 4. This may confirm the reliability in measuring ΔT by this method. The values of $\Delta T/\Delta T_b$ for membranes o-m-2, o-m-3 and i-m-2 were 0.69, 0.71 and 0.70, respectively.

Therefore, by using this linear relationship, the effective temperature difference ΔT during thermoosmosis can be estimated from the bulk temperature difference ΔT_b without measuring the thermal membrane potential. Moreover, the ratio $\Delta T/\Delta T_b$ for the uncharged membrane c-m may be assumed to be equal to that for membrane o-m-2 since both membranes have the same thickness.

3.2. Thermal hydrostatic pressure difference and hydraulic permeation

The difference between two solution levels was set to zero at the beginning of measurements of the thermal hydrostatic pressure difference. After 3–6 h the thermal hydrostatic pressure difference reached a constant value. The relationship between the thermal hydrostatic pressure difference and the effective temperature difference for membrane o-m-3 is shown in fig. 5. It is observed that the pressure difference is proportional to the effective temperature difference and all lines converge at the origin. The level of the cold solution was lower than that of the hot solution at the steady state.

Fig. 6 shows the hydraulic permeation velocities of various solutions as a function of the pressure dif-

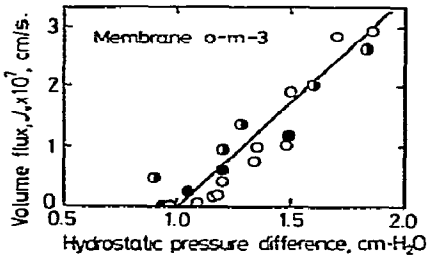

Fig. 6. Hydraulic permeations through membrane o-m-3. KCl concentrations (mol/kg): ●, 0.003; ◐, 0.02; ○, 0.75.

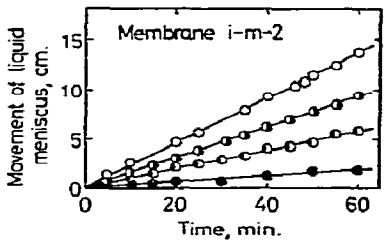

Fig. 7. Examples of the movement of liquid meniscus in capillary with time at four temperature differences, ΔT, in 0.02 mol/kg KCl solution with membrane i-m-2. The diameter of the capillary was 0.098 cm. ΔT(K): ○, 11.7; ◑, 10.1; ◐, 8.4; ●, 6.6.

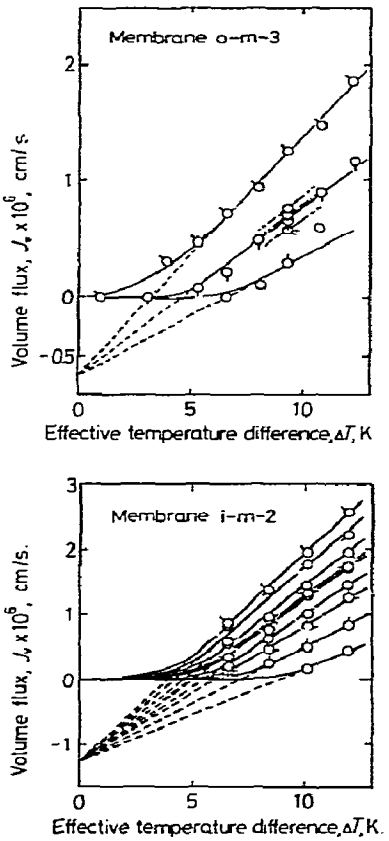

Fig. 8. The dependence of thermoosmotic flow on effective temperature difference (a) with membrane o-m-3, (b) with i-m-2. KCl concentration (mol/kg): ○, 0.001; ◇, 0.003; ○-, 0.01; ♀, 0.02; -○, 0.05; ♂, 0.1; ♀, 0.2; ♂, 0.35 for (a) and 0.5 for (b); ♁, 0.75 for (a) and 0.93 for (b).

ference. The hydraulic permeation did not occur until a finite head difference was given between solutions on both sides of the membrane.

3.3. Thermal volume flow

A long induction period of 0.5–6 h was required for movement of the meniscus in the capillary in measuring thermal volume flow. In general, the induction period was short when the thermoosmotic flow velocity was high. The induction period could be caused by bending of the membrane and/or an additional friction in the membrane, though the membrane was fixed with three thin plates of resin. However, after the meniscus began to move, the meniscus moved linearly with time as shown in fig. 7. At a given experimental condition, the reproducibility was very good, though the induction period was not constant.

The thermoosmotic volume flux J_v can be determined from the slope in fig. 7. The flux is plotted against effective temperature difference in fig. 8. Similar experimental results for membranes o-m-2 and c-m were reported previously [10]. The direction of thermoosmotic flow was from the cold side to the hot side in all experiments. Some workers reported that the thermoosmosis is proportional to the temperature difference ΔT [4,5]. In the present work, however, such proportionality was observed, only above a finite temperature difference as seen in fig. 8.

By combining the data in figs. 5 and 6, we can also calculate the water flux which would occur due to temperature difference. For example, the water fluxes at $\Delta T = 10$ K estimated by the above method are 5.1×10^{-5} and 7.3×10^{-5} cm/min for 0.02 and 0.75 mol/kg KCl solutions, respectively, which are comparable to 4.6×10^{-5} and 8.3×10^{-5} cm/min measured directly. Considering the experimental error, the agreement between these values is satisfactory. Thus, it may be concluded that all graphs in fig. 8 must converge at a point below zero, as shown in the figure. That is, an unknown constant resistance, such as surface tension, the force to bend the membrane etc., must be overcome to observe the flow of solution in thermoosmosis. Comparing the experimental errors in both measurements of hydrostatic pressure difference and thermal volume flow, we employed the latter method to determine the thermoosmotic coefficient.

3.4. Thermoosmotic coefficient

From the above experimental results, we may conclude that the rate of thermoosmosis J_v is proportional to the temperature difference ΔT

$$-J_v = D\Delta T, \tag{6}$$

where it is assumed that D is positive if the flow occurs from the hot side to the cold side.

The slopes D determined for membrane o-m-3 and i-m-2 in fig. 8, together with the data for membranes

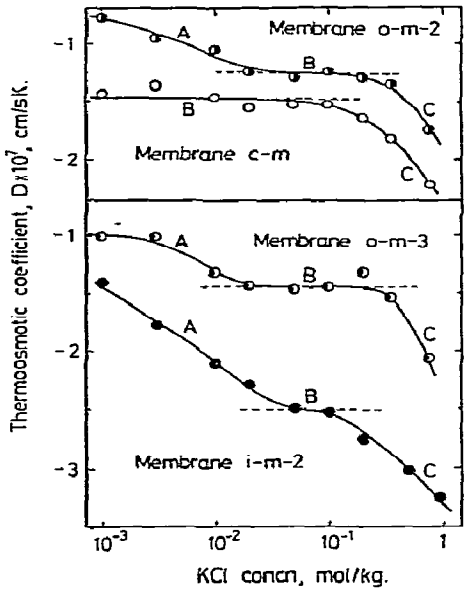

Fig. 9. The dependence of the thermoosmotic coefficient, D, on KCl concentration for membranes o-m-2, o-m-3, c-m and i-m-2.

o-m-2 and c-m reported previously [10], are plotted against KCl concentration in fig. 9. It can be observed that the dependence of D on electrolyte concentration of all charged membranes o-m-2, o-m-3 and i-m-2 appears to be made of three parts A, B and C.

Although no theoretical analysis of the data in fig. 9 is available at this time, the shape of the curves may by qualitatively reasonable: In thermoosmosis, through uncharged membrane c-m, the absolute magnitude of thermoosmosis increases as the concentration of electrolyte increases. This may be so because the flow of electrolyte through the membrane increases and, thereby, accelerates the flow of water with increasing concentration of electrolyte. Moreover, the absolute value of the thermoosmotic coefficient of uncharged membrane c-m is higher than that of membrane o-m-2 which was prepared by oxidation of membrane c-m. Since the driving force is the same in both cases, the difference may be caused by an additional resistance of fixed charges and counterions in o-m-2. Therefore, the effect of charges of the membrane on thermoosmosis is observed in part A of fig. 9. The absolute value of the thermoosmotic coefficient is decreased due to the effect of counterions of the membrane but the effect may disappear at high concentrations of electrolyte. In the ranges B and C, therefore, there would be no effect of charges and the curves for c-m and o-m-2 should overlap each other. The difference between the two curves observed in practice in fig. 9 may be caused by additional effects of electrolyte on the membrane structure. If the membrane has a high charge density like membrane i-m-2, the effect of charges on thermoosmosis is observed over a wide range of electrolyte concentrations and, hence, the ranges A, B and C cannot clearly be separated as can be seen in fig. 9.

In this work, both electrolyte and water move from the cold side to the hot side, whereas electrolyte moves from the hot side to the cold side in ordinary thermal diffusion experiments. However, this may not be a contradiction. The flow of electrolyte is observed relative to water in ordinary thermal diffusion experiments, whereas in thermoosmosis, the solution levels on both sides of the membrane are kept equal so that both electrolyte and water can move freely. Here, it is to be noted that the change in the electrolyte concentration in the cold chamber was too small to be detected by measuring the electrical conductivity of the solution. That is, the direction of electrolyte flow relative to the membrane is clearly from the cold side to the hot side, but that relative to water is not clear.

The present experimental results are in agreement with those of Dariel and Kedem [7] and Goldstein and Verhoff [8], but in disagreement with those of Carr and Sollner [4].

References

[1] H.J.V. Tyrrell, D.A. Taylor and C.M. Williams, Nature 177 (1956) 668.
[2] M. Tasaka, S. Morita and M. Nagasawa, J. Phys. Chem. 69 (1965) 4191.
[3] M. Tasaka, K. Hanaoka, Y. Kurosawa and C. Wada, Biophys. Chem. 3 (1975) 331; 4 (1976) 214.
[4] C.W. Carr and K. Sollner, J. Electrochem. Soc. 109 (1962) 616.
[5] H. Voellmy and P. Läuger, Ber. Bunsenges. Physik. Chem. 70 (1966) 165.
[6] R. Haase and H.J. de Greiff, Z. Naturforsch. 26a (1971) 1773.

[7] M.S. Dariel and O. Kedem, J. Phys. Chem. 79 (1975) 336.
[8] W.E. Goldstein and F.H. Verhoff, A.I.Ch.E.J. 21 (1975) 229.
[9] R. Haase and H.J. de Greiff, Z. Phys. Chem. (Frankfurt) 44 (1965) 301.
[10] M. Tasaka and M. Nagasawa, J. Polymer Sci. Symp. 49 (1975) 31.
[11] K. Sollner, I. Abrams and C.W. Carr, J. Gen. Physiol. 25 (1941) 7;
C.W. Carr and K. Sollner, J. Gen. Physiol. 28 (1944) 119;
H.P. Gregor and K. Sollner J. Phys. Chem. 50 (1946) 53.
[12] M. Tasaka, Y. Kondo and M. Nagasawa, J. Phys. Chem. 73 (1969) 3181.